

Supplementary Material

Bi-directional Charge Transfer Channels in Highly Crystalline Carbon Nitride Enabling Superior Photocatalytic Hydrogen Evolution

Runlu Liu,^a Siyuan Liu,^a Jingyi Lin,^a Xiaoxiao Zhang,^a Yao Li,^a Hui Pan,^a Lingti Kong,^a Shenmin Zhu,^{*a} John Wang^{*b}

^a State Key Laboratory of Metal Matrix Composites, School of Materials Science and Engineering, Shanghai Jiao Tong University, Shanghai 200240, China.

^b Department of Materials Science and Engineering, National University of Singapore, Singapore 117574, Singapore.

*Corresponding authors:

Email addresses: smzhu@sjtu.edu.cn (S. Zhu), msewangj@nus.edu.sg (J. Wang).

Experimental

1. Synthesis of photocatalysts

1.1 *Synthesis of carbon nitride (DCN) by self-assembly* Carbon nitride was prepared by a self-assembly method in dimethyl sulfoxide (DMSO). Typically, 1 g of melamine and 1 g of cyanuric acid was dissolved in 40 ml and 20 ml DMSO, denoted as solution A and B, respectively. The two solutions were then mixed and kept stirring for 4 hours. Subsequently, the mixture was centrifuged to remove the liquid and obtain the white precursor, denoted as MC. It was then washed with water and ethanol and dried at 60°C, before the MC was put into a crucible with a cover and then calcinated

at 550°C for 4 h in N₂ atmosphere (ramping rate 2.3°C/min). The obtained sample was denoted as DCN.

1.2 Synthesis of D-A-structured carbon nitride with K intercalation (TCCN-K) by self-assembly The precursor of TCCN-K was synthesized by the same procedure as DCN, except that 0.2 g of 2,5-Thiophenedicarboxylic acid (2,5-TDCA) was added into solution B. The precursor of TCCN-K, denoted as MCT, was mixed with KCl (weight ratio 1:5) and fully grinded, and then calcinated at 550°C for 4 h in N₂ atmosphere (ramping rate 2.3°C/min). After cooling down to room temperature, the dark yellow powder was washed with deionized water and ethanol for several times and then freeze-dried. The obtained sample was denoted as TCCN-K.

1.3 Synthesis of D-A-structured carbon nitride (TCCN) by self-assembly TCCN was obtained by soaking TCCN-K in boiling deionized water to remove the intercalated K ions.

1.4 Synthesis of D-A-structured carbon nitride with K intercalation (KTCCN) by direct calcination 2 g of melamine, 0.2 g of 2,5-TDCA and 10 g of KCl were mixed and fully grinded. The mixture was then calcinated at 550°C for 4 h in N₂ atmosphere (ramping rate 2.3°C/min). After cooling down to room temperature, the dark yellow powder was washed with deionized water and ethanol for several times and then freeze-dried. The obtained sample was denoted as KTCCN.

1.5 Synthesis of bulk carbon nitride (BCN) by direct calcination 2 g of melamine was calcinated at 550°C for 4 h in N₂ atmosphere (ramping rate 2.3°C/min). After cooling down to room temperature, the light yellow bulk was grinded into powder, denoted as BCN.

2. Characterizations

The morphology of each sample was observed by using scanning electron microscopy (SEM, Hitachi S-4800) and transmission electron microscopy (TEM, Talos F200X G2) equipped with an energy-dispersive X-ray spectrometer (EDS). The N₂ adsorption-desorption test was conducted on a Micromeritics 3Flex sorption

apparatus. The crystal structure of the samples was confirmed by X-ray powder diffraction (XRD) using a Rigaku D/max 2550VL/PC system. Fourier transform infrared (FT-IR) spectra were acquired on a Thermo Scientific Nicolet 6700 FT-IR Spectrometer. Solid-state ^{13}C nuclear magnetic resonance (NMR) spectra of the samples were acquired on a Bruker AVANCE NEO 600 MHz solid-state NMR spectrometer at room temperature. X-ray Photoelectron Spectra (XPS) of the samples were collected on a K-Alpha X-ray photoelectron spectrometer (Thermo Scientific) equipped with Al $K\alpha$ monochromatized radiations at 1486.6 eV as the X-ray source. The binding energies were referred to as the C 1s peak (284.8 eV) from adventitious carbon. Ultraviolet-Visible (UV-Vis) adsorption spectra of the samples were collected with a Perkin-Elmer Lambda 950 UV-Vis-NIR spectrophotometer. Photoluminescence (PL) spectra and time-resolved photoluminescence (TR-PL) spectra were collected on an Edinburgh FLS1000 photoluminescence spectrometer with an excitation wavelength at 365 nm. The room temperature electron paramagnetic resonance (EPR) spectra were acquired by a Bruker A300 electron paramagnetic resonance spectrometer. Hall effect test was conducted on an Ecopia HMS-7000 device. Certain amount of sample powder was pressed into tablets of 5 * 5 * 0.7 mm. The parameters were measured under a magnetic field of 0.5 T and electric current of 10⁻⁶ mA at 300K. The interlayer electrical conductivity and resistivity of TCCN-K and TCCN were measured using an ST2722-SD four-point probe powder resistivity tester.

3. Photoelectrochemical measurements

The transient photocurrent responses and electrochemistry impedance spectroscopy (EIS) were performed on an electrochemical workstation (CHI 600E) with a standard three electrode cell system, where an indium tin oxide (ITO) glass substrate deposited with the above samples, a platinum wire and an Ag/AgCl electrode serve as the working electrode, counter electrode and reference electrode,

respectively, and a 0.5 M Na₂SO₄ solution was used as the electrolyte. The working electrode was prepared by a dip-coating method.

4. Photocatalytic hydrogen evolution

The test of photocatalytic hydrogen production reaction was carried out in an online photocatalytic hydrogen production system (LabSolar-3AG, PerfectLight, Beijing). A 300 W Xe lamp with a cut-off filter ($\lambda > 420$ nm) was used as the visible light source. In detail, 20 mg of the as-prepared sample was dispersed in an aqueous solution (50 mL of water and 10 mL of TEOA as the hole sacrificial agent), and 3wt% Pt as the co-catalyst was loaded on the surface of catalyst by *in-situ* photodeposition method using 154 μ L of 20 mM H₂PtCl₆·6H₂O solution. The mixture solution was continuously stirred by a magnetic stirrer. Before visible light irradiation, the reactant system was cooled to ca. 5°C by recirculating cooling water and thoroughly degassed to remove air. The amount of hydrogen evolved was analyzed by a gas chromatograph (A91 Plus, Panna, Shanghai) equipped with a thermal conductivity detector and Ar as carrier gas. The apparent quantum efficiency (AQE) was examined under the same condition as activity evaluations, except that the 420 nm cut-filter was substituted by a band-pass filter (420, 435, 450, 475 nm, $\lambda \pm 10$ nm at 10% of peak height). The AQE was quantified with the following formula:

$$AQE = \frac{\text{number of reacted electrons}}{\text{number of incident photons}} = \frac{\alpha \times M \times N_A \times h \times c}{S \times P \times t \times \lambda} \times 100\%$$

where $\alpha = 2$ for the PHE reaction, M is the amount of hydrogen molecules (mol), N_A is Avogadro constant (6.02×10^{23} mol⁻¹), h is Planck constant (6.626×10^{-34} J·s), c is the light speed (3×10^8 m/s), S is the irradiation area (cm²), P is the irradiation intensity (W/cm²), t is the reaction time (s), and λ is the wavelength of monochromatic light (m).

5. Computational details

The Vienna Ab Initio Simulation Package (VASP) was employed to perform spin polarized density functional theory (DFT) calculations within the generalized gradient approximation (GGA) using the PBE formulation¹⁻³. The projected augmented wave (PAW) potentials were adopted to describe the nucleus-electron interaction, using a plane wave basis set with a kinetic energy cutoff of 450 eV^{4,5}. Partial occupancies of the Kohn–Sham orbitals were allowed using the Gaussian smearing method and a width of 0.05 eV. The electronic and ionic convergence criteria were taken as 10^{-6} eV and 0.01 eV/Å, respectively. Grimme’s DFT-D3 methodology was used to describe the dispersion interactions⁶. A $3 \times 2 \times 1$ Γ -centered k-mesh was used for the Brillouin zone integration for the supercell ($10 \times 16 \times 20$ Å). The K^+ doped structure was simulated with a TCCN bilayer with the doping ion locating in between the layers.

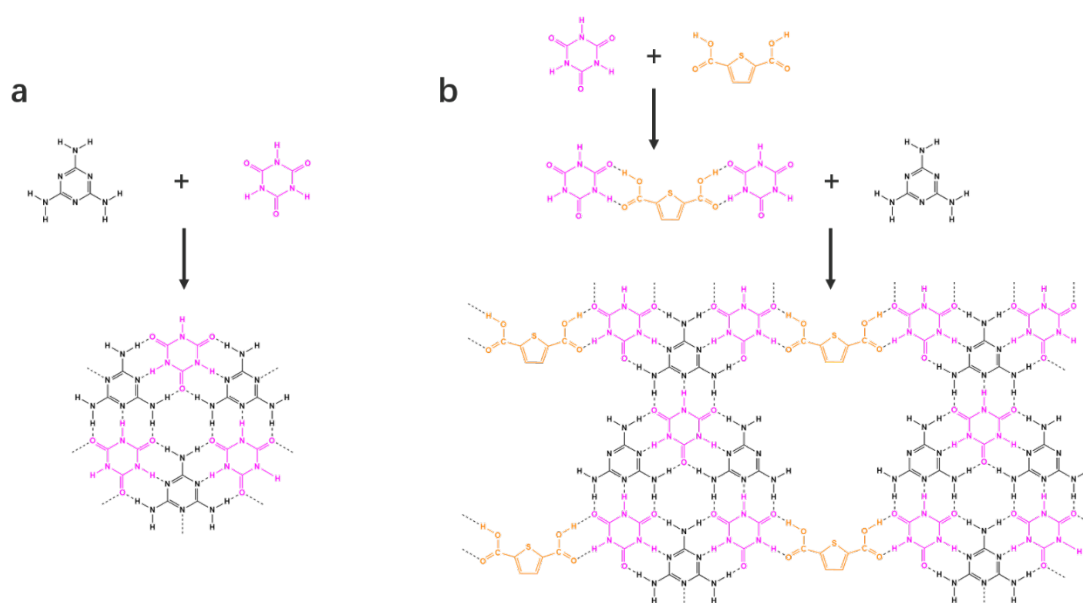


Fig. S1. The schematic diagram of self-assembly process of MC (a) and MCT (b).

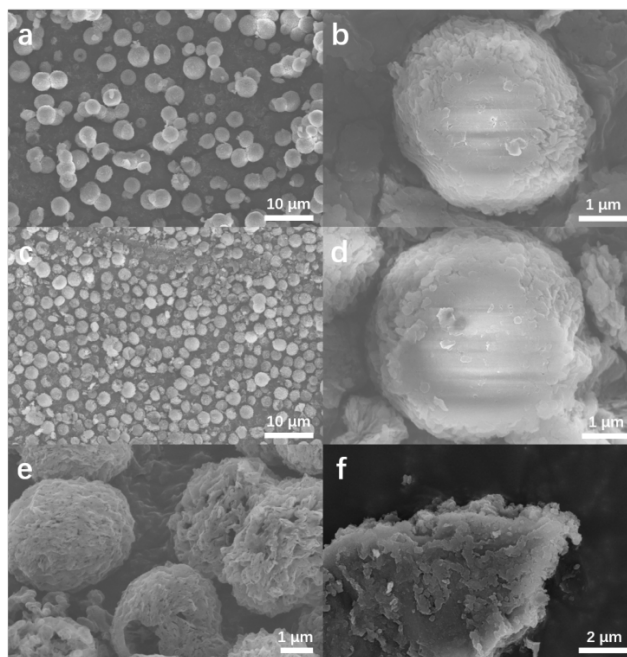


Fig. S2. SEM images of MCT (a, b), MC (c, d), DCN (e) and KTCCN (f).

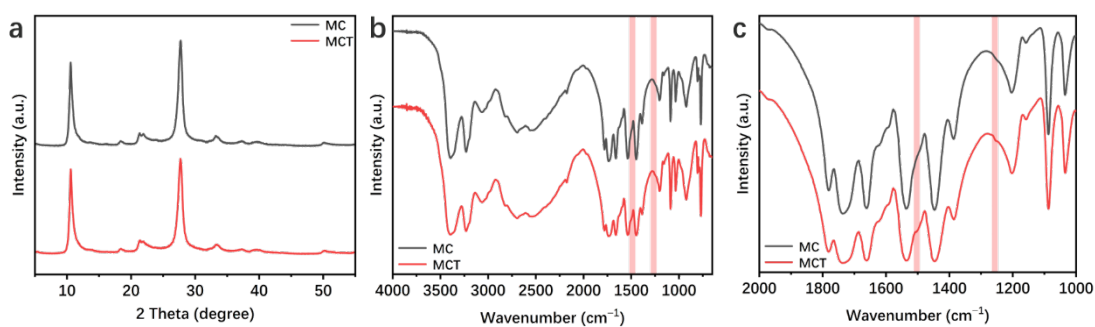


Fig. S3. XRD patterns (a) and FT-IR spectra (b) of MC and MCT.

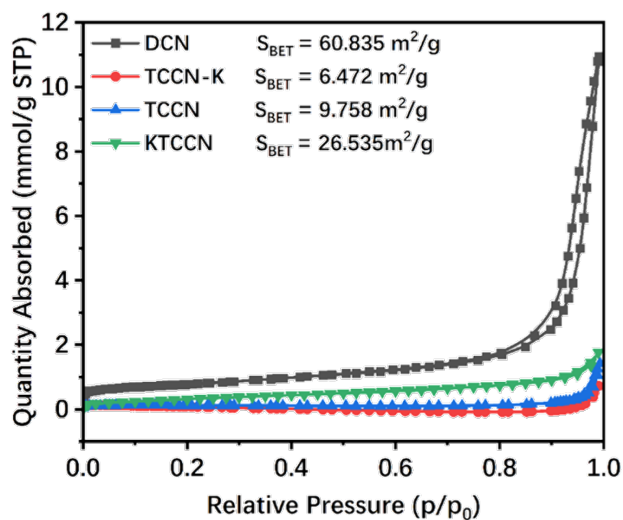


Fig. S4. N₂ adsorption-desorption curves and corresponding BET specific surface area of DCN, TCCN-K, TCCN and KTCCN.

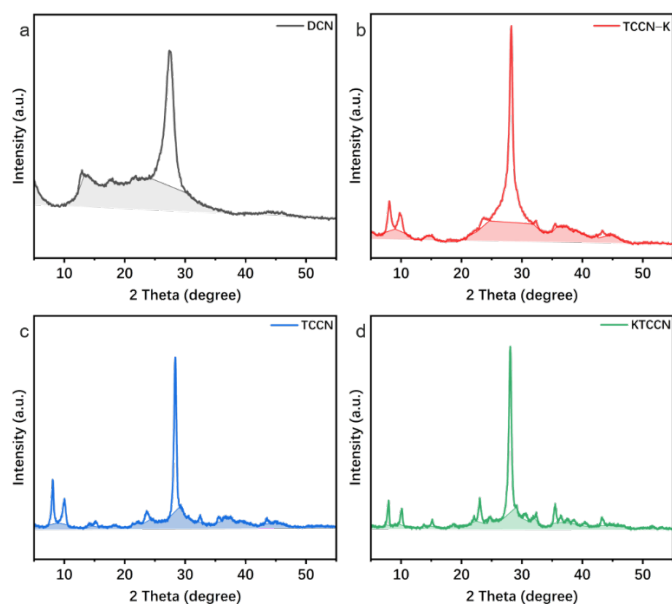


Fig. S5. The crystallinity of DCN, TCCN-K, TCCN and KTCCN.

Sample	I_c	I_a
DCN	0.336	0.664
TCCN-K	0.462	0.538
TCCN	0.438	0.562
KTCCN	0.390	0.610

Table S1. The relative integral peak intensity of crystal peaks (I_c) and amorphous peaks (I_a) of the samples.

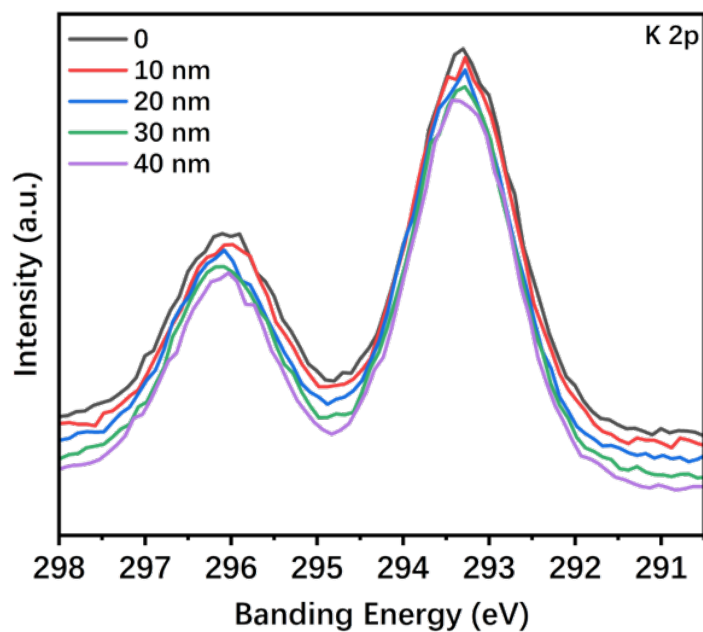


Fig. S6. In-depth XPS spectra of K 2p of the TCCN-K sample.

Etching depth (nm)	K concentration
0	11.28
10	12.33
20	11.91
30	12.18
40	12.42

Table S2. The concentration of K ions at different depth of TCCN-K sample measured from in-depth XPS spectra.

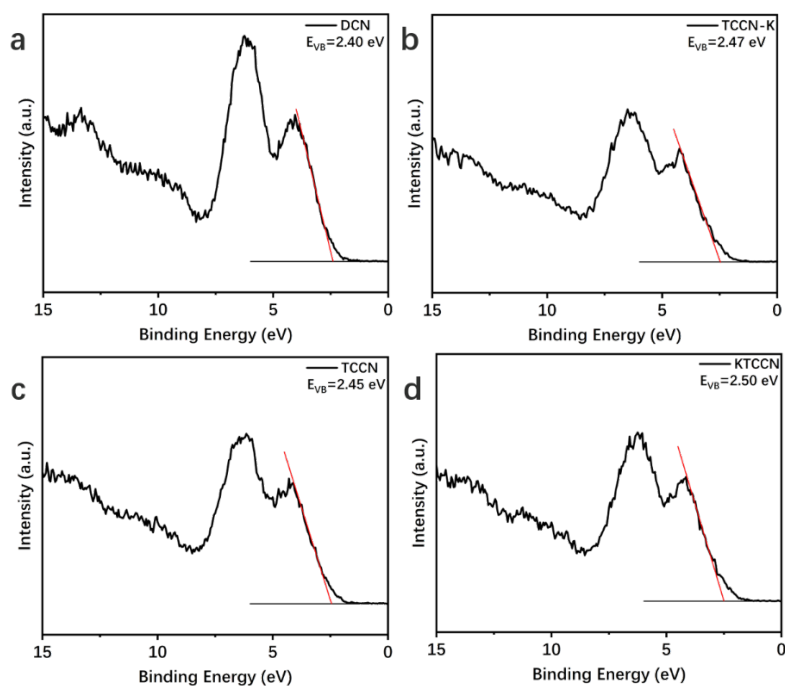


Fig. S7. XPS valence band spectra of CN (a), TCCN-K (b), TCCN (c) and KTCCN (d).

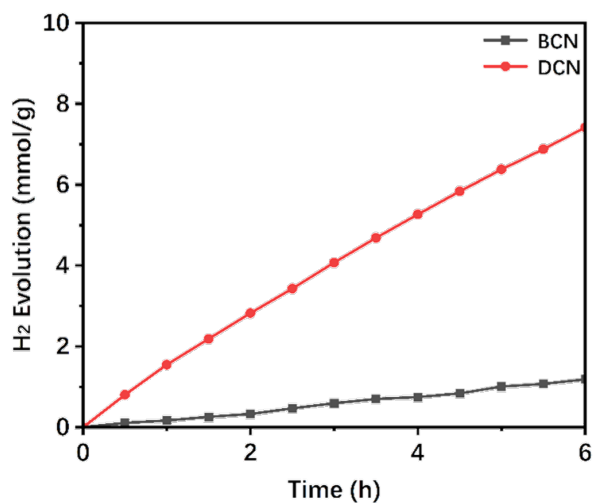


Fig. S8. Time courses of BCN and DCN for photocatalytic hydrogen evolution

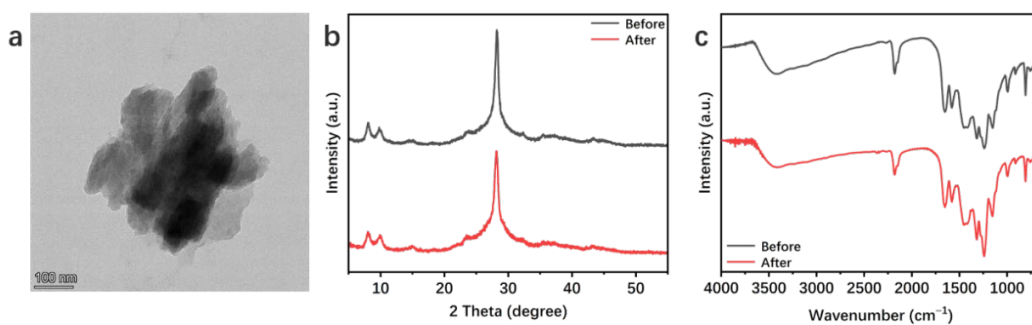


Fig. S9. TEM image (a), XRD pattern (b) and FT-IR spectrum (c) of TCCN-K after 24 hours' cycling test.

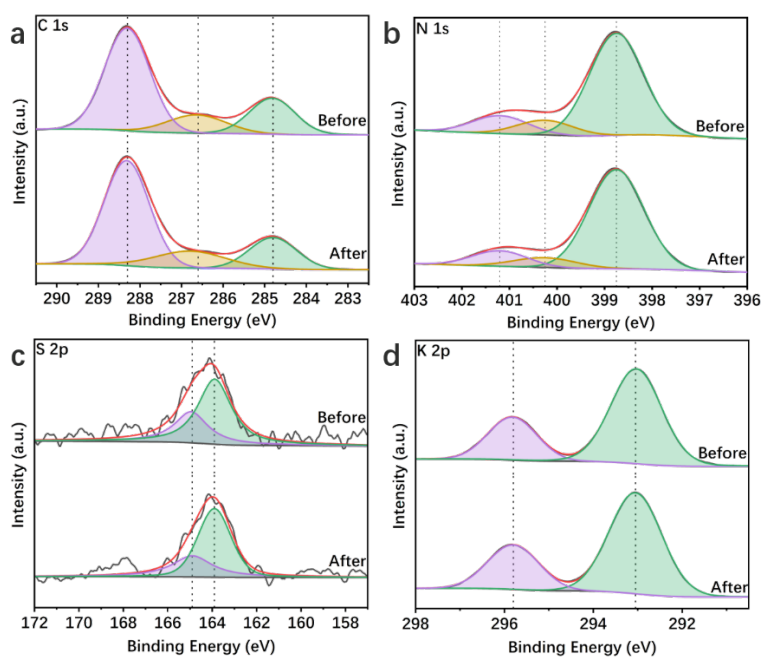


Fig. S10. C 1s (a), N 1s (b), S 2p (c) and K 2p (d) XPS spectra of TCCN-K after 24 hours' cycling test.

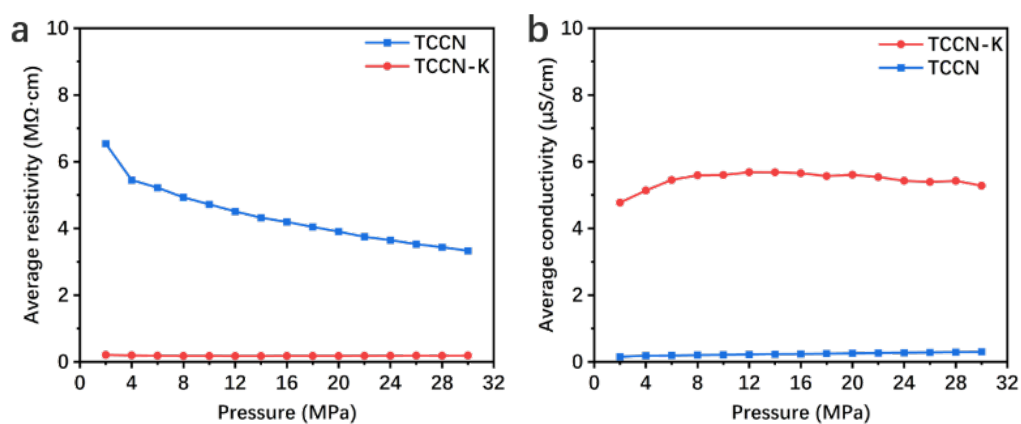


Fig. S11. The average interlayer electrical resistivity (a) and conductivity (b) of TCCN and TCCN-K under different pressure.

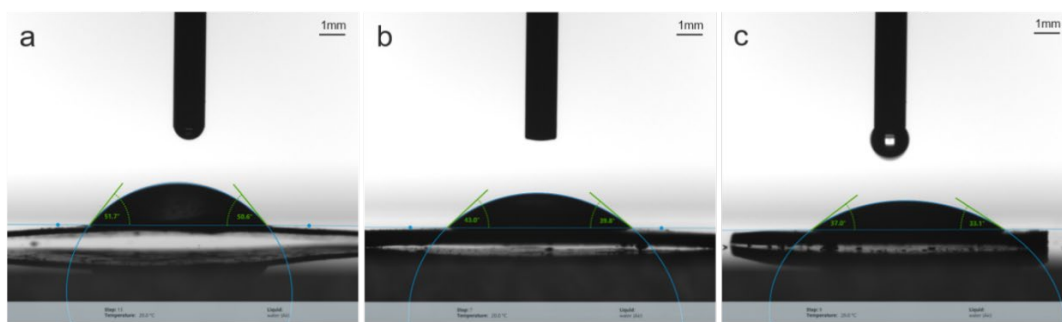


Fig. S12. The static contact angles of a water droplet (ca. 1 mL) on DCN (a), TCCN (b) and TCCN-K (c).

Catalysts	Catalyst mass	Co-catalysts	Light source	HER rate ($\mu\text{mol h}^{-1} \text{g}^{-1}$)	Improved ratio	Ref.
Donor- π -acceptor-type carbon nitride	20 mg	1wt % Pt	300 W Xe lamp > 420 nm	2881	5.1	7
Donor- π -acceptor- π -donor structured carbon nitride	50 mg	3wt % Pt	300 W Xe lamp > 420 nm	3428	5.9	8
Donor-acceptor structured carbon nitride	20 mg	2wt % Pt	300 W Xe lamp > 420 nm	3638	3.8	9
Intramolecular g- C_3N_4 -based donor-acceptor conjugated copolymers	50 mg	3wt % Pt	300 W Xe lamp > 420 nm	3613	8.9	10
Carbon nitride and dibenzothiophene dioxide-based intramolecular donor-acceptor conjugated copolymers	50 mg	3wt % Pt	300 W Xe lamp > 420 nm	5020	8.5	11
Benzene-ring-incorporated g- C_3N_4	50 mg	3wt % Pt	300 W Xe lamp > 420 nm	2791	8.2	12
Donor-acceptor conjugated polymer/g- C_3N_4 heterojunction	50 mg	\	300 W Xe lamp > 420 nm	13000	17.8	13

Indenofluorene-containing donor-acceptor conjugated polymer dots/g-C ₃ N ₄ nanosheets heterojunction	20mg	Co-catalyst free	300 W Xe lamp > 420 nm	181.1	\	¹⁴
Donor-acceptor structured carbon nitride	20 mg	3wt % Pt	300 W Xe lamp > 420 nm	7449	6.0	This work

Table S3. Comparison of the similar type C₃N₄-based photocatalysts for hydrogen evolution.

References

1. G. Kresse and J. Furthmüller, *Phys. Rev. B*, 1996, **54**, 11169-11186.
2. J. P. Perdew, K. Burke and M. Ernzerhof, *Phys. Rev. Lett.*, 1996, **77**, 3865-3868.
3. G. Kresse and D. Joubert, *Phys. Rev. B*, 1999, **59**, 1758-1775.
4. P. E. Blöchl, *Phys. Rev. B*, 1994, **50**, 17953-17979.
5. S. Grimme, J. Antony, S. Ehrlich and H. Krieg, *J. Chem. Phys.*, 2010, **132**, 154104.
6. G. Henkelman, B. P. Uberuaga and H. Jónsson, *J. Chem. Phys.*, 2000, **113**, 9901-9904.
7. Z. Sun, Y. Jiang, L. Zeng and L. Huang, *ChemSusChem*, 2019, **12**, 1325-1333.
8. K. Li and W. D. Zhang, *Small*, 2018, **14**, e1703599.
9. C. Zhu, T. Wei, Y. Wei, L. Wang, M. Lu, Y. Yuan, L. Yin and L. Huang, *J. Mater. Chem. A*, 2021, **9**, 1207-1212.
10. H. Che, C. Liu, G. Che, G. Liao, H. Dong, C. Li, N. Song and C. Li, *Nano Energy*, 2020, **67**.
11. F. Yu, Z. Wang, S. Zhang, W. Wu, H. Ye, H. Ding, X. Gong and J. Hua, *Nanoscale Adv.*, 2021, **3**, 1699-1707.
12. R. Jiang, G. Lu, J. Liu, D. Wu, Z. Yan and Y. Wang, *Renew. Energy*, 2021, **164**, 531-540.
13. F. Yu, Z. Wang, S. Zhang, H. Ye, K. Kong, X. Gong, J. Hua and H. Tian, *Adv. Funct. Mater.*, 2018, **28**.
14. W. Zhou, T. Jia, D. Zhang, Z. Zheng, W. Hong and X. Chen, *Appl. Catal. B: Environ.*, 2019, **259**.